# Reconciling LSND and Super-Kamiokande data through the dynamical Lorentz symmetry breaking in a four-Majorana fermion model

Y. M. P. Gomes[1,*] and M. J. Neves[2,†]

[1]*Departamento de Física Teórica, Universidade do Estado do Rio de Janeiro, 20550-013 Rio de Janeiro, Brazil*

[2]*Departamento de Física, Universidade Federal Rural do Rio de Janeiro, BR 465-07, 23890-971 Seropédica, Rio de Janeiro, Brazil*

(Received 24 January 2022; accepted 4 July 2022; published 15 July 2022)

We propose a model of Majorana fermions with quartic self-couplings. These Majorana fermions acquire masses via a type-II seesaw mechanism in which the physical eigenstates are identified as a light Majorana fermion and another heavy Majorana fermion. On a physical basis, the quartic self-couplings involve axial currents of these Majorana fermions, and also the interaction of the axial current for the light particle with the heavy particle one. We introduce two auxiliaries gauge fields in this model, and we study the stability conditions of the correspondent effective potential of the model. The ground state of the effective potential introduces two 4-vectors as scales of vacuum expected values, and consequently, the dynamical Lorentz symmetry breaking (DLSB) emerges in the model. We use the expansion of the effective action to calculate the effective Lagrangian up to second order in the auxiliary fields as fluctuations around the ground state. This mechanism generates dynamics for the auxiliary gauge fields, mixed mass terms, longitudinal propagation, and Chern-Simons term through radiative corrections. After the diagonalization, the two gauge fields gain masses through an analogous type-II seesaw mechanism in which a gauge boson has a light mass, and the other one acquires a heavy mass. In this scenario of Lorentz symmetry breaking, we obtain the correspondent dispersion relations for the Majorana fermions and the gauge boson fields. Posteriorly, we analyze the neutrino's oscillations in the presence of a DLSB parameter, in the transition $\nu_e \to \nu_\mu$. We discuss the parameter space of this transition and show that the DLSB can conciliate the LSND and Super-Kamiokande results.

DOI: 10.1103/PhysRevD.106.015013

## I. INTRODUCTION

The Standard Model (SM) is the most successful framework to describe the interaction among the elementary particles at the electroweak (EW) scale. However, many experimental features indicate the SM as an effective theory and it must be part of a more fundamental theory. The neutrino's oscillation phenomena measure the squared difference of the neutrinos masses and indicate that the SM needs to be extended to include masses for the neutrinos [1]. The difference squared of neutrino's masses is associated with the observed probability transition $\nu_\mu \to \nu_e$ reported by the LSND experiment [2–9].

Several mechanisms to generate masses to the neutrinos are known in the literature [10–15]. The most famous is the seesaw mechanism in which right-handed neutrinos (RHNs) are introduced in models beyond the SM to provide the largest particle content with a rich phenomenology that can be detected in accelerators in the future. In these extended models, the scalar sector after the spontaneous symmetry breaking (SSB) yields masses to the left-handed neutrinos (LHNs) (light mass), and the right-handed neutrinos (heavy mass). This is known as a type-II seesaw mechanism. Some phenomenological models involving Lorentz symmetry breaking have been proposed as well [16–18].

In the context of Majorana particles, is well known that the possibilities for built fermionic bilinears are constrained due to Majorana conditions. For instance, with one Majorana spinor, there are only three possibilities, which are the scalar, pseudoscalar, and pseudovectorial (axial) bilinears [19]. One can use these bilinears to form quartic interactions, and through both perturbative and nonperturbative approaches, one can show that these models are a rich environment to dynamical symmetry breaking (DSB) occurs [20–24]. Interestingly, one can analyze one special

*yurimullergomes@gmail.com
†mariojr@ufrrj.br

four-fermion interaction for Majorana particles—the axial one. As can be seen in Refs. [25–30] the axial four-fermion interaction can dynamically generate the breaking of the Lorentz symmetry by the non-null vacuum expected value (VEV) of the axial bilinear $\langle\bar{\psi}\gamma^{\mu}\gamma_5\psi\rangle \neq 0$, and therefore the vacuum state of the model violates the Lorentz symmetry, and also the $CP$ and $CPT$ symmetries.

In this paper, we propose a model with two Majorana fermions that couple through the quartic interactions. After a type-II seesaw mechanism, in the physical field basis, one Majorana fermion acquires a light mass (that can describe a light neutrino), while the other one has a heavy mass that can be fixed at a high energy scale. On a physical basis, the Majorana fermions have two axial quartic self-coupling, and the third coupling involves the axial current of the light fermion contracted with the axial current of the heavy-fermion at the tree level. This model is an extension of the 4D Thirring model with a light fermion and another heavy-fermion that couple between itself through quartic interactions. However, this model is not renormalizable. It must be thought of as a low-energy effective theory and as part of a more fundamental theory. In this sense, the proposal is analogous to the Nambu-Jona-Lasinio (NJL) model for QCD [24].

We introduce two auxiliaries gauge fields to obtain the effective potential of the model. The ground state of the model is obtained in terms of two constant 4-vectors where the effective potential is minimized. We examine the behavior of the model around these two vacuum expected values (VEVs) to generate radiative contributions to the action. We calculate the radiative corrections up to second-order to obtain the propagation terms for the auxiliaries gauge bosons. The massive terms generated are mixed and depend on the Majorana masses from the seesaw mechanism: one gauge field has a light mass, while another one has a heavy mass. Since the mixing is very weak, a term Chern-Simons term appears associated with the heavy gauge field. As a consequence of these radiative corrections, the Lorentz and $CPT$ symmetry is broken spontaneously. Therefore, we obtain the correspondent dispersion relations for the Majorana fermions and gauge bosons comparing them with the results already known in the literature. As an application of the seesaw mechanism, we also examine the neutrino oscillations calculating the transition probability of $\nu_e \to \nu_\mu$, and the oscillation length in the strong quartic coupling limit. We discuss the influence of the DLSB in the parameter space of this transition.

The paper is organized as follows. In Sec. II, we review the type-II seesaw mechanism and propose the most general quartic couplings for two Majorana fermions. Section III focuses on the effective model in which are introduced two auxiliaries gauge fields, and we obtain the effective potential and the dispersion relations for the Majorana fermions with an LSV scenario. In Sec. IV, we calculate the effective Lagrangian up to second-order and the dispersion relations for the gauge bosons induced by the field fluctuations around the ground state of the model. Section V is dedicated to the application of the neutrino's oscillations in which we examine the probability in the transition $\nu_e \to \nu_\mu$ and we obtain the parameter space. Our conclusions and final remarks are cast in Sec. VI.

We adopt the convention for the metric $\eta^{\mu\nu} = \mathrm{diag}(+1,-1,-1,-1)$, and we work with the natural units: $\hbar = c = 1$.

## II. THE DESCRIPTION OF THE FOUR-MAJORANA MODEL

In many models with Majorana neutrinos in the literature, the mass sector with left-handed neutrinos $(\nu_L)$ and right-handed neutrinos $(N_R)$ is given by

$$-\mathcal{L}_{\mathrm{mass}} = M\bar{\nu}_L N_R + M_L\overline{\nu_L^c}\nu_L + M_R\overline{N_R^c}N_R + \mathrm{H.c.}, \tag{1}$$

where $M$ are $3\times 3$ matrix elements of Dirac mass term, $M_L$ are $3\times 3$ matrix elements of a Majorana mass term for LHNs, and $M_R$ is the correspondent one to RHNs. The $\nu_L$ sets a column of three LHNs, *i. e.*, $\{\nu_{eL},\nu_{\mu L},\nu_{\tau L}\}$, and $N_R$ is the similar column vector for the RHNs. For a brief review, a four-component Majorana fermion is defined as a spinor $\psi$ which obeys the identity $\psi \equiv \psi^c = i\gamma^2\psi^*$. The counterpart $\overline{\psi^c}$ is given by $\overline{\psi^c} = \psi^t C$, where $C = i\gamma^0\gamma^2$ is the unitary charge conjugation matrix $C^\dagger = C^{-1}$, $\psi^t$ means the transpose column matrix for the $\psi$-spinor, and $\{\gamma^0,\gamma^2\}$ are two Dirac matrices. Backing to the mass sector (1), it is defined the variables $\eta := \nu_L + \nu_L^c$ and $\chi := N_R + N_R^c$, the massive Lagrangian can be written in terms of the two four-component Majorana spinors $\eta$ and $\chi$:

$$\begin{aligned}-\mathcal{L}_{\mathrm{mass}} &= \frac{M}{2}(\bar{\eta}\chi + \bar{\chi}\eta) + M_L\bar{\eta}\eta + M_R\bar{\chi}\chi \\ &= (\bar{\eta}\quad\bar{\chi})\begin{bmatrix} M_L & M/2 \\ M/2 & M_R\end{bmatrix}\begin{pmatrix}\eta\\ \chi\end{pmatrix}.\end{aligned} \tag{2}$$

The mass eigenstates, that we denote by $\psi_i$ $(i = 1, 2)$, are obtained by the diagonalization of the mass matrix:

$$\psi_1 = \cos\theta\eta - \sin\theta\chi, \tag{3a}$$

$$\psi_2 = \sin\theta\eta + \cos\theta\chi, \tag{3b}$$

where $\tan 2\theta = \frac{M}{M_L - M_R}$, and the correspondent eigenvalues are given by:

$$m_1 = \frac{1}{2}(M_L + M_R) - \frac{1}{2}\sqrt{(M_L - M_R)^2 + M^2}, \tag{4a}$$

$$m_2 = \frac{1}{2}(M_L + M_R) + \frac{1}{2}\sqrt{(M_L - M_R)^2 + M^2}. \tag{4b}$$

The condition $M_R \gg M_L \gg M$ is applied for the neutrino's case. Under this consideration, the previous eigenvalues are read below:

$$m_1 \simeq M_L - \frac{M^2}{4M_R} \simeq M_L, \tag{5a}$$

$$m_2 \simeq M_R + \frac{M^2}{4M_R} \simeq M_R, \tag{5b}$$

and the mixing angle is very small $\theta \simeq -M/(2M_R) \ll 1$, where we can write $\cos\theta \simeq 1$ and $\sin\theta \simeq 0$ in (3a) and (3b). Thereby, $\psi_1$ is identified as a light Majorana fermion (left-handed neutrinos), and $\psi_2$ is a heavy Majorana fermion that describes a right-handed neutrino with mass defined on the TeV scale or higher.

For one Majorana $\psi$-spinor, the nontrivial bilinears which can be formed are: $\bar{\psi}\psi$, $\bar{\psi}\gamma_5\psi$, and $\bar{\psi}\gamma^\mu\gamma_5\psi$. Otherwise, any bilinear combination is null. Using the properties of the Majorana spinors, the nontrivial bilinear involving $\eta$ and $\chi$ are the combinations below:

$$\bar{\eta}\gamma^\mu\gamma_5\eta, \quad \bar{\chi}\gamma^\mu\gamma_5\chi, \quad \bar{\chi}\gamma^\mu\gamma_5\eta + \bar{\eta}\gamma^\mu\gamma_5\chi, \quad \bar{\eta}\gamma^\mu\chi - \bar{\chi}\gamma^\mu\eta. \tag{6}$$

Following these combinations, we propose the most general pseudovector quartic self-interaction for the Majorana fermions $\eta$ and $\chi$:

$$\mathcal{L}^{\text{int}} = \frac{G_1}{2}(\bar{\eta}\gamma_\mu\gamma_5\eta)^2 + \frac{G_2}{2}(\bar{\chi}\gamma_\mu\gamma_5\chi)^2 + \frac{G_3}{2}(\bar{\eta}\gamma_\mu\gamma_5\chi + \bar{\eta}\gamma_\mu\gamma_5\chi)^2 + \frac{G_4}{2}(\bar{\eta}\gamma_\mu\chi - \bar{\chi}\gamma_\mu\eta)^2, \tag{7}$$

where $G_i$ $(i = 1, 2, 3, 4)$ are coupling constants with length dimension squared. Using the Fierz identities

$$\frac{1}{4}(\bar{\eta}\gamma_\mu\chi - \bar{\chi}\gamma_\mu\eta)^2 = (\bar{\eta}\eta)(\bar{\chi}\chi) - (\bar{\eta}\gamma_5\eta)(\bar{\chi}\gamma_5\chi) - \frac{1}{2}(\bar{\eta}\gamma_\mu\gamma_5\eta)(\bar{\chi}\gamma^\mu\gamma_5\chi), \tag{8a}$$

$$\frac{1}{4}(\bar{\eta}\gamma_\mu\gamma_5\chi + \bar{\eta}\gamma_\mu\gamma_5\chi)^2 = -(\bar{\eta}\eta)(\bar{\chi}\chi) + (\bar{\eta}\gamma_5\eta)(\bar{\chi}\gamma_5\chi) - \frac{1}{2}(\bar{\eta}\gamma_\mu\gamma_5\eta)(\bar{\chi}\gamma^\mu\gamma_5\chi), \tag{8b}$$

the couplings from (7) are written in the physical eigenstates basis $\{\psi_1, \psi_2\}$ as:

$$\mathcal{L}^{\text{int}} = -\frac{G_1}{2}(\bar{\psi}_1\gamma_\mu\gamma_5\psi_1)^2 - \frac{G_2}{2}(\bar{\psi}_2\gamma_\mu\gamma_5\psi_2)^2 + \frac{1}{2}(G_3 + G_4)(\bar{\psi}_1\gamma_\mu\gamma_5\psi_1)(\bar{\psi}_2\gamma^\mu\gamma_5\psi_2) - (G_3 - G_4)[(\bar{\psi}_1\psi_1)(\bar{\psi}_2\psi_2) - (\bar{\psi}_1\gamma_5\psi_1)(\bar{\psi}_2\gamma_5\psi_2)], \tag{9}$$

where we have considered the small mixing angle. We choose the case in which $G_3 = G_4$, such that the NJL-like terms that could contribute with the dynamically generated masses can be eliminated, and we will focus just in the terms with the axial currents of $\psi_1$ and $\psi_2$. In this particular case, the couplings are read:

$$\mathcal{L}^{\text{int}} = -\frac{G_1}{2}(\bar{\psi}_1\gamma_\mu\gamma_5\psi_1)^2 - \frac{G_2}{2}(\bar{\psi}_2\gamma_\mu\gamma_5\psi_2)^2 + G_3(\bar{\psi}_1\gamma_\mu\gamma_5\psi_1)(\bar{\psi}_2\gamma^\mu\gamma_5\psi_2). \tag{10}$$

Therefore, the model contains axial couplings for description of the processes $\psi_1\psi_1 \to \psi_1\psi_1$, $\psi_2\psi_2 \to \psi_2\psi_2$, and $\psi_1\psi_1 \to \psi_2\psi_2$ at tree level. This is an extension of the model studied in Ref. [25], in which we will investigate the dynamical symmetry breaking.

## III. THE EFFECTIVE POTENTIAL AND THE DISPERSION RELATIONS FOR THE MAJORANA FERMIONS

We consider in this section the model with the two Majorana fermions and their quartic self-interactions through the axial currents:

$$\mathcal{L}_{\text{model}} = \bar{\psi}_1(i\partial\!\!\!/ - m_1)\psi_1 - \frac{G_1}{2}(\bar{\psi}_1\gamma_\mu\gamma_5\psi_1)^2 + \bar{\psi}_2(i\partial\!\!\!/ - m_2)\psi_2 - \frac{G_2}{2}(\bar{\psi}_2\gamma_\mu\gamma_5\psi_2)^2 + G_3(\bar{\psi}_1\gamma_\mu\gamma_5\psi_1)(\bar{\psi}_2\gamma^\mu\gamma_5\psi_2). \tag{11}$$

This Lagrangian is equivalent to

$$\mathcal{L}_{\text{model}} = \bar{\psi}_1(i\partial\!\!\!/ - gA\!\!\!/\gamma_5 - m_1)\psi_1 + \bar{\psi}_2(i\partial\!\!\!/ - g'B\!\!\!/\gamma_5 - m_2)\psi_2 + \frac{1}{2}g_1^2A_\mu A^\mu + \frac{1}{2}g_2^2B_\mu B^\mu + g_3^2A_\mu B^\mu, \tag{12}$$

where the auxiliary fields $A^\mu$ and $B^\mu$, using the motion equations, satisfy the constraints

$$A^\mu = \frac{g_2^2}{g_1^2g_2^2 - g_3^4}\left[g\bar{\psi}_1\gamma^\mu\gamma_5\psi_1 - \frac{g_3^2}{g_2^2}g'\bar{\psi}_2\gamma^\mu\gamma_5\psi_2\right], \tag{13a}$$

$$B^\mu = \frac{g_1^2}{g_1^2g_2^2 - g_3^4}\left[g'\bar{\psi}_2\gamma^\mu\gamma_5\psi_2 - \frac{g_3^2}{g_1^2}g\bar{\psi}_1\gamma^\mu\gamma_5\psi_1\right], \tag{13b}$$

and the coupling constants $G_i$ $(i=1, 2, 3)$ are parametrized by

$$G_1 := \frac{g^2g_2^2}{g_1^2g_2^2 - g_3^4}, \quad G_2 := \frac{g^2g_1^2}{g_1^2g_2^2 - g_3^4} \quad \text{and} \quad G_3 := \frac{gg'g_3^2}{g_1^2g_2^2 - g_3^4}. \tag{14}$$

Notice also that the constants $g_i$ $(i = 1, 2, 3)$ have mass dimension, while that $g$ and $g'$ are dimensionless coupling constants of the fermions $\psi_1$ and $\psi_2$, with the auxiliary gauge fields $A^\mu$ and $B^\mu$, respectively. The perturbative formalism allow us to define the functional integration

$$Z = \int \mathcal{D}A^\mu \mathcal{D}B^\mu \mathcal{D}\bar{\psi}_1 \mathcal{D}\psi_1 \mathcal{D}\bar{\psi}_2 \mathcal{D}\psi_2 e^{i\int d^4x \mathcal{L}_{\text{model}}} = \int \mathcal{D}A^\mu \mathcal{D}B^\mu e^{iS_{\text{eff}}(A,B)}, \tag{15}$$

where, after the fermion integrations, we obtain the effective action

$$S_{\text{eff}}(A,B) = \int d^4x \left[\frac{1}{2}g_1^2 A^2 + \frac{1}{2}g_2^2 B^2 + g_3^2 A\cdot B\right] - i\text{Tr}\ln(i\partial\!\!\!/ - gA\!\!\!/\gamma_5 - m_1) - i\text{Tr}\ln(i\partial\!\!\!/ - g'B\!\!\!/\gamma_5 - m_2), \tag{16}$$

and Tr means the trace on the Dirac matrices and on the coordinate, or on the momentum space. The correspondent effective potential is

$$V_{\text{eff}}(A,B) = -\frac{1}{2}g_1^2 A^2 - \frac{1}{2}g_2^2 B^2 - g_3^2 A\cdot B + i\int \frac{d^4p}{(2\pi)^4}\text{tr}[\ln(p\!\!\!/ - m_1 - gA\!\!\!/\gamma_5)] + i\int \frac{d^4p}{(2\pi)^4}\text{tr}[\ln(p\!\!\!/ - m_2 - g'B\!\!\!/\gamma_5)]. \tag{17}$$

This potential has two nontrivial minimals:

$$\left.\frac{\partial V_{\text{eff}}}{\partial A_\mu}\right|_{A=\alpha,B=\beta} = -g_1^2\alpha^\mu - g_3^2\beta^\mu + i\Pi_1^\mu = 0, \tag{18a}$$

and

$$\left.\frac{\partial V_{\text{eff}}}{\partial B_\mu}\right|_{A=\alpha,B=\beta} = -g_2^2\beta^\mu - g_3^2\alpha^\mu + i\Pi_2^\mu = 0, \tag{18b}$$

where

$$\Pi_1^\mu = \int \frac{d^4p}{(2\pi)^4}\text{tr}\left[\frac{1}{p\!\!\!/ - m_1 - \phi\!\!\!/\gamma_5}(-g)\gamma^\mu\gamma_5\right], \tag{19a}$$

$$\Pi_2^\mu = \int \frac{d^4p}{(2\pi)^4}\text{tr}\left[\frac{1}{p\!\!\!/ - m_2 - b\!\!\!/\gamma_5}(-g')\gamma^\mu\gamma_5\right], \tag{19b}$$

and we have defined $a^\mu = g\alpha^\mu$, e $b^\mu = g'\beta^\mu$. Both integrals are like the tadpole diagrams and diverge in the ultraviolet limit. We introduce the dimensional regularization (with a $D$ regulator parameter) to calculate these integrals, and consequently, we can isolate the divergent terms. The coupling constants $g$ and $g'$ are replaced by $g \to g(\mu^2)^{1-d/2}$ and $g' \to g'(\mu^2)^{1-d/2}$, where $\mu$ is an arbitrary energy scale. After some manipulations, the trace calculus yields the regularized integrals

$$\Pi_1^\mu(D) = -4g(\mu^2)^{1-d/2}\int \frac{d^Dp}{(2\pi)^D} \times \frac{2[-p^2a^\mu + (p\cdot a)p^\mu] + (p^2 - m_1^2 - a^2)a^\mu}{(p^2 - m_1^2 - a^2)^2 + 4[p^2a^2 - (p\cdot a)^2]}, \tag{20}$$

$$\Pi_2^\mu(D) = -4g'(\mu^2)^{1-d/2}\int \frac{d^Dp}{(2\pi)^D} \times \frac{2[-p^2b^\mu + (p\cdot b)p^\mu] + (p^2 - m_2^2 - b^2)b^\mu}{(p^2 - m_2^2 - b^2)^2 + 4[p^2b^2 - (p\cdot b)^2]}. \tag{21}$$

Using the approximation $\{m_1^2, m_2^2\} \gg \{a^2, b^2\}$, we expand the previous integral into the $a$ and $b$-parameters to obtain the results

$$i\Pi_1^\mu = ga^\mu\left[\frac{m_1^2}{\pi^2\epsilon} - \frac{m_1^2}{\pi^2}\ln\left(\frac{m_1}{\Lambda}\right) + \frac{a^2}{3\pi^2}\right], \tag{22a}$$

$$i\Pi_2^\mu = g'b^\mu\left[\frac{m_2^2}{\pi^2\epsilon} - \frac{m_2^2}{\pi^2}\ln\left(\frac{m_2}{\Lambda}\right) + \frac{b^2}{3\pi^2}\right], \tag{22b}$$

where we have used the physical dimension in $D = 4 - \epsilon$, and $\Lambda^2 := 4\pi\mu^2 e^{-\gamma}$, in which $\gamma = 0.577$ is the Euler-Mascheroni constant. Therefore, we substitute these results in (18b) and (18b), respectively, and we obtain the relations:

$$\frac{g_3^2}{gg'}b^\mu = a^\mu\left[-\frac{g_1^2}{g^2} + \frac{m_1^2}{\pi^2\epsilon} - \frac{m_1^2}{\pi^2}\ln\left(\frac{m_1}{\Lambda}\right) + \frac{a^2}{3\pi^2}\right], \tag{23a}$$

$$\frac{g_3^2}{gg'}a^\mu = b^\mu\left[-\frac{g_2^2}{g'^2} + \frac{m_2^2}{\pi^2\epsilon} - \frac{m_2^2}{\pi^2}\ln\left(\frac{m_2}{\Lambda}\right) + \frac{b^2}{3\pi^2}\right]. \tag{23b}$$

From the above equations, we have two nontrivial solutions:

(1) Phase I—The case of $b^\mu = 0$, the solution for $a^\mu \neq 0$ is given by

$$-\frac{g_{1R}^2}{g^2} - \frac{m_1^2}{\pi^2}\ln\left(\frac{m_1}{\Lambda}\right) + \frac{a^2}{3\pi^2} = 0. \tag{24}$$

(2) Phase II—For the case of $a^\mu = 0$ and $b^\mu \neq 0$, the solution is

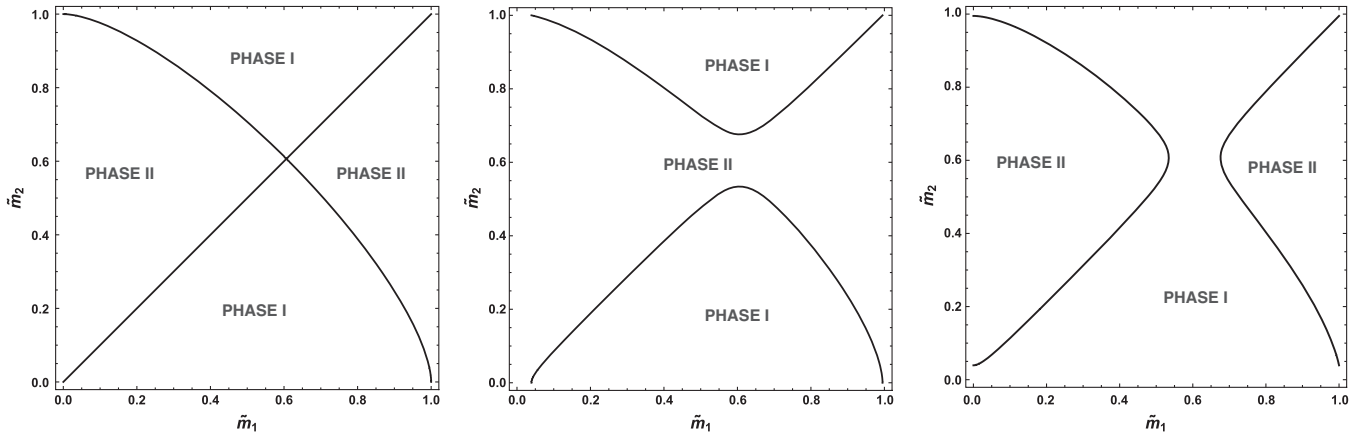


FIG. 1. The phase diagram of the model for $G_3 \neq 0$, with the conditions $G_2 > G_1$ (left panel), $G_1 = G_2$ (middle panel) and $G_1 > G_2$ (right panel), respectively. The phase I refers to the region in which $\beta^\mu = 0$ and $\alpha^\mu \neq 0$, while the phase II region correspond to $\alpha^\mu = 0$ and $\beta^\mu \neq 0$. The masses are normalized in energy scale unit.

$$-\frac{g_{2R}^2}{g'^2} - \frac{m_2^2}{\pi^2}\ln\left(\frac{m_2}{\Lambda}\right) + \frac{b^2}{3\pi^2} = 0. \tag{25}$$

The phase space is illustrated in the Fig. 1 including the three cases: $G_2 > G_1$ (right panel), $G_2 = G_1$ (middle panel), and $G_1 > G_2$ (right panel). We use $G_3 \neq 0$ in all plots. The masses $(\tilde{m}_1, \tilde{m}_2)$ are normalized by the energy scale $(\mu)$, i.e., $\tilde{m}_i \equiv m_i/\mu$ $(i = 1, 2)$.

It is important to highlight that only in the case $g_3 = 0$, both pseudovectors can acquire non-null vacuum expected values. Notice that, in both solutions, we have defined the renormalizable coupling constants

$$\frac{g_{1R}^2}{g^2} = \frac{g_1^2}{g^2} - \frac{m_1^2}{\pi^2\epsilon} \quad \text{and} \quad \frac{g_{2R}^2}{g'^2} = \frac{g_2^2}{g'^2} - \frac{m_2^2}{\pi^2\epsilon}. \tag{26}$$

The true solution of the gap equation is defined by the global minimum of the potential. Integrating the gap equations, we obtain the effective potential:

$$V_{\text{eff}}(A,B) = \frac{g^2}{12\pi^2}(A^2 - a^2)^2 + \frac{g'^2}{12\pi^2}(B^2 - b^2)^2 - g_3^2 A\cdot B. \tag{27}$$

Thereby, true minimum of the potential is at the points

$$a^2 = 3\pi^2\left[\frac{g_{1R}^2}{g^2} + \frac{m_1^2}{\pi^2}\ln\left(\frac{m_1}{\Lambda}\right)\right] \quad \text{and} \quad b^\mu = 0, \tag{28a}$$

$$b^2 = 3\pi^2\left[\frac{g_{2R}^2}{g'^2} + \frac{m_2^2}{\pi^2}\ln\left(\frac{m_2}{\Lambda}\right)\right] \quad \text{and} \quad a^\mu = 0. \tag{28b}$$

If we consider a very small mass for $\psi_1$-Majorana fermion, the first minimum point is determinate by the renormalized coupling constant $g_{1R}$, i.e., $a^2 = 3\pi^2 g_{1R}^2/g^2$. The effective potential has a nontrivial minimal in which $\langle A^\mu\rangle = \alpha^\mu$ and $\langle B^\mu\rangle = \beta^\mu$ are two scales of VEVs that break the Lorentz symmetry.

As consequence, the modified dispersion relations for the Majorana fermions are read below. In the phase I:

$$(p^2 - m_1^2 - a^2)^2 + 4[p^2a^2 - (p\cdot a)^2] = 0, \tag{29a}$$

$$p^2 = m_2^2, \tag{29b}$$

and in the phase II:

$$p^2 = m_1^2, \tag{30a}$$

$$(p^2 - m_2^2 - b^2)^2 + 4[p^2b^2 - (p\cdot b)^2] = 0. \tag{30b}$$

These dispersion relations are analogous to Carroll-Field-Jackiw-Proca electrodynamics [31]. The frequency solutions from (29a) and (30b) are hard to obtain in this present form. Thus, we can consider the particular cases of a timelike and spacelike DLSB parameter. For a timelike case, in which $a^\mu = (a^0, \mathbf{0})$ and $b^\mu = (b^0, \mathbf{0})$, the frequency solutions are read below:

$$\omega_1^{(\pm)}(\mathbf{p}) = \sqrt{(|\mathbf{p}| \pm a_0)^2 + m_1^2} \simeq ||\mathbf{p}| \pm a_0| + \frac{m_1^2}{2||\mathbf{p}| \pm a_0|}, \tag{31}$$

and

$$\omega_2^{(\pm)}(\mathbf{p}) = \sqrt{(|\mathbf{p}| \pm b_0)^2 + m_2^2} \simeq m_2 + \frac{(|\mathbf{p}| \pm b_0)^2}{2m_2}. \tag{32}$$

For the spacelike case, where $a^\mu = (0, \mathbf{a})$ and $b^\mu = (0, \mathbf{b})$, the frequency solutions are given by

$$\omega_1^{(\pm)}(\mathbf{p}) = \sqrt{\mathbf{p}^2 + m_1^2 + \mathbf{a}^2 \pm 2|\mathbf{a}|\sqrt{m_1^2 + (\mathbf{p}\cdot\hat{\mathbf{a}})^2}} \simeq |\mathbf{p} \pm \mathbf{a}| + \frac{m_1^2}{2|\mathbf{p} \pm \mathbf{a}|}, \tag{33}$$

and

$$\omega_2^{(\pm)}(\mathbf{p}) = \sqrt{\mathbf{p}^2 + m_2^2 + \mathbf{b}^2 \pm 2|\mathbf{b}|\sqrt{m_2^2 + (\mathbf{p}\cdot\hat{\mathbf{b}})^2}} \simeq m_2 \pm |\mathbf{b}| + \frac{\mathbf{p}^2}{2m_2}. \tag{34}$$

We have considered the condition from the seesaw mechanism $m_2 \gg m_1$ in the previous approximation. For the massless case, for example, if we consider $\psi_1$ a Majorana fermion with a very small mass in which we can neglect it $m_1 \approx 0$ with a generic DLSB parameter, the frequencies are given by

$$\omega_1^{\pm}(\mathbf{p}) = -a_0 \pm |\mathbf{p} + \mathbf{a}|, \tag{35a}$$

$$\omega_2^{\pm}(\mathbf{p}) = a_0 \pm |\mathbf{p} - \mathbf{a}|. \tag{35b}$$

The usual RDs are recovered when $a^\mu \to 0$. Other important point is that the results (35a) reproduce asymmetric frequencies and it depend on the direction of the vector $\mathbf{a}$ with a propagation direction $\hat{\mathbf{p}}$.

## IV. THE EFFECTIVE ACTION

The vacuum properties of the model help us to understand the dynamics of the fluctuations dictated by the auxiliary fields $A^\mu$ and $B^\mu$. Thereby, we expand these auxiliary fields around the vacuum minimal as: $A^\mu(x) = \alpha^\mu + X^\mu(x)$ and $B^\mu(x) = \beta^\mu + Y^\mu(x)$, respectively, where $X^\mu$ and $Y^\mu$ are interpreted as the new dynamical fields of the model, and $\{\alpha^\mu, \beta^\mu\}$ do not depend on the space-time coordinates. The effective action in terms of $X^\mu$ and $Y^\mu$ is

$$\begin{aligned} S_{\text{eff}}(X,Y) = \int d^4x \Big\{ & \frac{1}{2}g_1^2\alpha^2 + \frac{1}{2}g_2^2\beta^2 \\ & + g_3^2(\alpha\cdot\beta) + X\cdot(g_1^2\alpha + g_3^2\beta) + Y\cdot(g_2^2\beta + g_3^2\alpha) \\ & + \frac{1}{2}g_1^2X^2 + \frac{1}{2}g_2^2Y^2 + g_3^2(X\cdot Y) \\ & - i\int \frac{d^4p}{(2\pi)^4}\mathrm{tr}[\ln(\not{p} - m_1 - \not{\alpha}\gamma_5 - g\not{X}\gamma_5)] \\ & - i\int \frac{d^4p}{(2\pi)^4}\mathrm{tr}[\ln(\not{p} - m_2 - \not{\beta}\gamma_5 - g'\not{Y}\gamma_5)] \Big\}. \end{aligned} \tag{36}$$

Now, we expand the previous effective action in power series of $X^\mu$ and $Y^\mu$, such that:

$$S_{\text{eff}}(X,Y) = \sum_{n=1}^{\infty} S^{(n)}(X,Y), \tag{37}$$

where the first correction ($n = 1$) is given by

$$\begin{aligned} S^{(1)}(X,Y) = i\int d^4x [ & X_\mu(i\Pi_1^\mu - g_1^2\alpha^\mu - g_3^2\beta^\mu) \\ & + Y_\mu(i\Pi_2^\mu - g_2^2\beta^\mu - g_3^2\alpha^\mu)] = 0. \end{aligned} \tag{38}$$

This contribution is null, as we expect, due to the relations (18b) and (18b). The self-energy term is the correction at the second order:

$$S^{(2)}(X,Y) = \frac{i}{2}\sum_{i,j=1}^{2}\int d^4x [V_\mu^i(x)\Pi_{ij}^{\mu\nu}V_\nu^j(x)], \tag{39}$$

where we have introduced the notation $V_\mu^i = (V_\mu^1, V_\mu^2) \equiv (X_\mu, Y_\mu)$, and the vacuum polarizations are given by

$$\Pi_{11}^{\mu\nu} = -i\eta^{\mu\nu}g_1^2 + \mathrm{Tr}[(-ig\gamma^\mu\gamma_5)S_1(p)(-ig\gamma^\nu\gamma_5)S_1(p-k)], \tag{40a}$$

$$\Pi_{12}^{\mu\nu} = \Pi_{21}^{\mu\nu} = -i\eta^{\mu\nu}g_3^2, \tag{40b}$$

$$\Pi_{22}^{\mu\nu} = -i\eta^{\mu\nu}g_2^2 + \mathrm{Tr}[(-ig'\gamma^\mu\gamma_5)S_2(p)(-ig'\gamma^\nu\gamma_5)S_2(p-k)], \tag{40c}$$

in which

$$S_1(p) = \frac{i}{\not{p} - m_1 - \not{\alpha}\gamma_5}, \tag{41a}$$

$$S_2(p) = \frac{i}{\not{p} - m_2 - \not{\beta}\gamma_5}. \tag{41b}$$

Since we know that $m_2 \gg m_1$ through the seesaw mechanism, we fix the $\psi_2$ mass at the energy scale ($\Lambda$), i.e., $m_2 \sim \Lambda$. In this case, the gap equations (23a) and (23b) are simplified to $a^2 \approx 3\pi^2 g_{1R}^2/g^2$, when $b^\mu = 0$, and $b^2 \approx 3\pi^2 g_{2R}^2/g'^2$, when $a^\mu = 0$, respectively. The global minima is defined for the condition $g_{1R} > g_{2R}$ in the first gap, and $g_{2R} > g_{1R}$ in the second gap. Since experimental measurements point out to a null or very small value for $|a^2|$ which couples with the SM neutrino, we can consider the condition $g_{2R} > g_{1R}$. Under these conditions, we obtain the vacuum polarizations in the position space

$$\Pi_{11}^{\mu\nu} = -i\eta^{\mu\nu}\left\{g_1^2 - \frac{g^2 m_1^2}{2\pi^2}\left[\frac{1}{\epsilon} - 2\ln\left(\frac{m_1}{\Lambda}\right)\right]\right\} - \frac{ig^2}{12\pi^2}\left[1 - \frac{1}{\epsilon} + 2\ln\left(\frac{m_1}{\Lambda}\right)\right](\eta^{\mu\nu}\Box - \partial^\mu\partial^\nu) - \frac{ig^2}{12\pi^2}\partial^\mu\partial^\nu, \tag{42a}$$

$$\Pi_{22}^{\mu\nu} = -i\eta^{\mu\nu}\left\{g_2^2 - \frac{g'^2 b^2}{\pi^2} - \frac{g'^2 m_2^2}{2\pi^2}\left[\frac{1}{\epsilon} - 2\ln\left(\frac{m_2}{\Lambda}\right)\right]\right\} - \frac{ig'^2}{12\pi^2}\left[1 - \frac{1}{\epsilon} + 2\ln\left(\frac{m_2}{\Lambda}\right)\right](\eta^{\mu\nu}\Box - \partial^\mu\partial^\nu) - \frac{ig'^2}{12\pi^2}\partial^\mu\partial^\nu + \frac{ig'^2}{12\pi^2}(b^\mu\partial^\nu - b^\nu\partial^\mu) - \frac{ig'^2}{4\pi^2}\left[\frac{1}{\epsilon} - 2\ln\left(\frac{m_2}{\Lambda}\right)\right]\epsilon^{\mu\nu\rho\sigma}b_\rho\partial_\sigma + \frac{g'^2}{4\pi^2}\left\{1 - \frac{9}{2}\left[\frac{1}{\epsilon} - 2\ln\left(\frac{m_2}{\Lambda}\right)\right]\right\}b^\mu b^\nu. \tag{42b}$$

Substituting these results in (39), we write the effective action as

$$S_{\text{eff}}^{(2)} = \int d^4x \mathcal{L}_{\text{eff}}^{(2)}, \tag{43}$$

where the renormalizable effective Lagrangian (at the second order) is given by

$$\mathcal{L}_{\text{eff}}^{(2)} = -\frac{1}{4}X_{R\mu\nu}^2 - \frac{g_R^2}{24\pi^2}(\partial_\mu X_R^\mu)^2 + \frac{1}{2}(6m_1^2)X_{R\mu}^2 - \frac{1}{4}Y_{R\mu\nu}^2 - \frac{g_R'^2}{24\pi^2}(\partial_\mu Y_R^\mu)^2 + \frac{1}{2}(6m_2^2)Y_{R\mu}^2 + g_{3R}^2 X_{R\mu}Y_R^\mu - \frac{g_R'^2}{12\pi^2}(b\cdot Y_R)\partial_\mu Y_R^\mu - \frac{27}{4}(b\cdot Y_R)^2 + \frac{3}{4}b_\mu\epsilon^{\mu\nu\rho\sigma}Y_{R\nu}Y_{R\rho\sigma}. \tag{44}$$

To get the effective Lagrangian in this form, we have defined the renormalized fields

$$X_R^\mu = Z_3^{-1/2}X^\mu, \qquad Y_R^\mu = Z_4^{-1/2}Y^\mu, \tag{45}$$

where the renormalization factors are given by

$$Z_3^{-1} = \frac{g^2}{12\pi^2}\left[1 - \frac{1}{\epsilon} + 2\ln\left(\frac{m_1}{\Lambda}\right)\right], \tag{46a}$$

$$Z_4^{-1} = \frac{g'^2}{12\pi^2}\left[1 - \frac{1}{\epsilon} + 2\ln\left(\frac{m_2}{\Lambda}\right)\right], \tag{46b}$$

and the renormalized coupling constants are

$$g_R = \sqrt{Z_3}g, \quad g_R' = \sqrt{Z_4}g', \quad g_{3R} = \sqrt[4]{Z_3Z_4}g_3. \tag{47}$$

The transversal operators from (42a) and (42b) induces dynamical for the auxiliary vector fields through the field strength tensors $X_{\mu\nu} = \partial_\mu X_\nu - \partial_\nu X_\mu$ and $Y_{\mu\nu} = \partial_\mu Y_\nu - \partial_\nu Y_\mu$, respectively. In (44), the correspondent renormalized field strength tensors are $X_{R\mu\nu} = Z_3^{-1/2}X_{\mu\nu}$, and $Y_{R\mu\nu} = Z_4^{-1/2}Y_{\mu\nu}$. Furthermore, in (44), the radiative corrections also induce a new Chern-Symons term depending on the $b^\mu$-parameter, $Y_R^\mu$ and the field strength tensor $Y_R^{\mu\nu}$. Note that, the effective Lagrangian also shows quadratic terms in $X_R^\mu$ and $Y_R^\mu$, and also a mixed term of $X_R^\mu$ with $Y_R^\mu$. These terms are interpreted as like-massive terms of the auxiliary fields $X_R$ and $Y_R$. We can write these terms into the matrix form

$$\mathcal{L}_{\text{mass}-XY}^{(2)} = \frac{1}{2}\eta^{\mu\nu}(V_{R\mu})^t M^2 V_{R\nu}, \tag{48}$$

in which $M^2$ is the mass matrix

$$M^2 = \begin{bmatrix} 6m_1^2 & g_{3R}^2 \\ g_{3R}^2 & 6m_2^2 \end{bmatrix}, \tag{49}$$

and $V_R^\mu$ is the column vector formed by the fields $X_R^\mu$ and $Y_R^\mu$. This mass matrix can be diagonalized by a $SO(2)$ matrix, say $\mathcal{R}$, in which transformations in the vector fields are

$$X_R^\mu = \cos\alpha Z_{1R}^\mu + \sin\alpha Z_{2R}^\mu, \tag{50a}$$

$$Y_R^\mu = -\sin\alpha Z_{1R}^\mu + \cos\alpha Z_{2R}^\mu, \tag{50b}$$

where $\alpha$ is a mixing angle, such that, $\tan(2\alpha) = g_{3R}^2/(3m_2^2 - 3m_1^2)$. The $Z_{1R}^\mu$ and $Z_{2R}^\mu$ are interpreted as the physical eigenstates for the auxiliary fields whose the masses are determinate by the diagonal matrix $M_D^2 = \mathcal{R}^t M^2 \mathcal{R} = \text{diag}(\mu_1^2, \mu_2^2)$, in which the eigenvalues $\{\mu_1^2, \mu_2^2\}$ are, respectively, read below

$$\mu_1^2 = 3(m_1^2 + m_2^2) - \sqrt{9(m_1^2 - m_2^2)^2 + g_{3R}^4} \simeq 6m_1^2 - \frac{g_{3R}^4}{6m_2^2}, \tag{51a}$$

$$\mu_2^2 = 3(m_1^2 + m_2^2) + \sqrt{9(m_1^2 - m_2^2)^2 + g_{3R}^4} \simeq 6m_2^2 + \frac{g_{3R}^4}{6m_2^2}, \tag{51b}$$

in which we have used the condition $m_2 \gg m_1$. Since that $m_2 \gg g_{3R}$, we identify $\mu_1 \simeq \sqrt{6}m_1$ as the $Z_{1R}$ mass eigenstate (light gauge boson), while that $\mu_2 \simeq \sqrt{6}m_2$ is the correspondent eigenstate for $Z_{2R}$ (heavy gauge boson). Under this condition, we can consider $\tan(2\alpha) \simeq g_{3R}^2/(3m_2^2) \ll 1$, such that $\sin\alpha \simeq g_{3R}^2/(6m_2^2) \simeq 0$ and $\cos\alpha \simeq 1$. In the $\{Z_{1R}, Z_{2R}\}$ basis, the effective Lagrangian (44) is

$$\mathcal{L}^{(2)}_{\text{eff}} = -\frac{1}{4}Z^2_{1R\mu\nu} + \frac{1}{2}\mu_1^2 Z^2_{1R\mu} - \frac{g_R^2}{24\pi^2}(\partial_\mu Z^\mu_{1R})^2 - \frac{1}{4}Z^2_{2R\mu\nu} + \frac{1}{2}\mu_2^2 Z^2_{2R\mu} - \frac{g_R'^2}{24\pi^2}(\partial_\mu Z^\mu_{2R})^2 - \frac{g_R'^2}{12\pi^2}(b\cdot Z_{2R})\partial_\mu Z^\mu_{2R} - \frac{27}{4}(b\cdot Z_{2R})^2 + \frac{3}{4}b_\mu \epsilon^{\mu\nu\rho\sigma} Z_{2R\nu} Z_{2R\rho\sigma}. \tag{52}$$

Notice that the Chern-Symons term emerges for the $Z^\mu_{2R}$ physical eigenstate when the mixing with the $Z^\mu_{1R}$ is very weak. The action principle yields the field equations:

$$\partial_\mu Z^{\mu\nu}_{1R} + \mu_1^2 Z^\nu_{1R} + \frac{g_R^2}{12\pi^2}\partial^\nu(\partial_\mu Z^\mu_{1R}) = 0, \tag{53a}$$

$$\partial_\mu Z^{\mu\nu}_{2R} + \mu_2^2 Z^\nu_{2R} + \frac{g_R'^2}{12\pi^2}\partial^\nu(\partial_\mu Z^\mu_{2R}) - \frac{g_R'^2}{12\pi^2}[b^\nu \partial_\mu Z^\mu_{2R} - \partial^\nu(b\cdot Z_{2R})] + \frac{3}{2}\epsilon^{\mu\nu\rho\sigma} b_\mu Z_{2R\rho\sigma} = 0. \tag{53b}$$

Operating $\partial_\nu$ on the Eqs. (53a) and (53b), the longitudinal part of $Z_{1R}$ and $Z_{2R}$ satisfies the relations

$$\left(\Box + \frac{12\pi^2\mu_1^2}{g_R^2}\right)\partial_\mu Z^\mu_{1R} = 0, \tag{54a}$$

$$\left(\Box - b\cdot\partial + \frac{12\pi^2\mu_2^2}{g_R'^2}\right)\partial_\mu Z^\mu_{2R} + \Box(b\cdot Z_{2R}) = 0. \tag{54b}$$

Substituting the plane wave solutions $Z^\mu_{iR}(x) = z^\mu_{iR}e^{ik\cdot x}$ $(i = 1, 2)$, in which $z^\mu_{iR}$ are the constant and uniform wave amplitudes, the equations (53a) and (53b) can be written as $M_1^{\mu\nu} z_{1R\mu} = 0$ and $M_2^{\mu\nu} z_{2R\mu} = 0$, respectively, where the matrices $M_i^{\mu\nu}$ $(i = 1, 2)$ are given by

$$M_1^{\mu\nu} = (-k^2 + \mu_1^2)\eta^{\mu\nu} + \left(1 - \frac{g_R^2}{12\pi^2}\right)k^\mu k^\nu, \tag{55a}$$

$$M_2^{\mu\nu} = (-k^2 + \mu_2^2)\eta^{\mu\nu} + \left(1 - \frac{g_R'^2}{12\pi^2}\right)k^\mu k^\nu + \frac{ig_R'^2}{12\pi^2}(b^\mu k^\nu - b^\nu k^\mu) + i3\epsilon^{\mu\nu\rho\sigma} b_\rho k_\sigma. \tag{55b}$$

The dispersion relations are determinate by the conditions $\det(M_1^{\mu\nu}) = 0$ and $\det(M_2^{\mu\nu}) = 0$. The null determinant of $M_1^{\mu\nu}$ yields the frequencies solutions $\omega^{(i)\pm}_{Z_{1R}} = \pm\omega^{(i)}_{Z_{1R}}(\mathbf{k})$ $(i = 1, 2)$, in which the dispersion relations $\omega^{(i)}_{Z_{1R}}(\mathbf{k})$ are read below:

$$\omega^{(1)}_{Z_{1R}}(\mathbf{k}) = \sqrt{\mathbf{k}^2 + \mu_1^2}, \tag{56a}$$

$$\omega^{(2)}_{Z_{1R}}(\mathbf{k}) = \sqrt{\mathbf{k}^2 + \frac{12\pi^2\mu_1^2}{g_R^2}}. \tag{56b}$$

The frequency (56a) is the transversal mode of $Z_{1R}$ with mass $\mu_1 = \sqrt{6}m_1$, and (56b) is the frequency associated with longitudinal propagation mode of $Z_{1R}$. For the case of $M_2^{\mu\nu}$, we assume a timelike vector $b^\mu = (b_0, \mathbf{0})$ in which four roots are possible for the null determinant: $\omega^{(i)\pm}_{Z_{2R}} = \pm\omega^{(i)}_{Z_{2R}}(\mathbf{k})$ $(i = 1, 2, 3, 4)$. These frequencies are given by

$$\omega^{(1)}_{Z_{2R}}(\mathbf{k}) = \sqrt{\mathbf{k}^2 - 3|b_0||\mathbf{k}| + \mu_2^2}, \tag{57a}$$

$$\omega^{(2)}_{Z_{2R}}(\mathbf{k}) = \sqrt{\mathbf{k}^2 + 3|b_0||\mathbf{k}| + \mu_2^2}, \tag{57b}$$

$$\omega^{(3)}_{Z_{2R}}(\mathbf{k}) = \sqrt{\mathbf{k}^2 + \frac{3\pi(g_R'^2 + 12\pi^2)\mu_2^2 - \sqrt{9\pi^2(g_R'^2 - 12\pi^2)^2\mu_2^4 - 3b_0^2 g_R'^6\mathbf{k}^2}}{6\pi g_R'^2}}, \tag{57c}$$

$$\omega^{(4)}_{Z_{2R}}(\mathbf{k}) = \sqrt{\mathbf{k}^2 + \frac{3\pi(g_R'^2 + 12\pi^2)\mu_2^2 + \sqrt{9\pi^2(g_R'^2 - 12\pi^2)^2\mu_2^4 - 3b_0^2 g_R'^6\mathbf{k}^2}}{6\pi g_R'^2}}. \tag{57d}$$

Notice that, when $b_0 \to 0$, the previous frequencies reduce to (56a) and (56b) exchanging $g_R' \to g_R$ and $\mu_2 \to \mu_1$.

Finally, we obtain the $n = 3$ contribution to the effective action, under the condition $a^\mu = 0$ and $b^\mu \neq 0$, is

$$\Pi^X_{\mu\nu\rho} = 0, \tag{58a}$$

$$\Pi^Y_{\mu\nu\rho} = \frac{ig'^3}{3\pi^2}(\beta_\mu\eta_{\nu\rho} + \beta_\nu\eta_{\nu\rho} + \beta_\rho\eta_{\mu\nu}). \tag{58b}$$

The divergent contribution vanishes due to the index symmetry. For the $n = 4$ contribution, one finds:

$$\Pi^{X}{}_{\mu\nu\rho\kappa} = \frac{ig^4}{3\pi^2}(\eta_{\mu\nu}\eta_{\rho\kappa} - \eta_{\mu\rho}\eta_{\nu\kappa} + \eta_{\mu\kappa}\eta_{\nu\rho}), \quad (59a)$$

$$\Pi^{Y}{}_{\mu\nu\rho\kappa} = \frac{ig'^4}{3\pi^2}(\eta_{\mu\nu}\eta_{\rho\kappa} - \eta_{\mu\rho}\eta_{\nu\kappa} + \eta_{\mu\kappa}\eta_{\nu\rho}). \quad (59b)$$

Again, the divergence vanishes due to the index symmetry. Therefore, using these results, the renormalized effective potential can be written in terms of the physical eigenstates $\{Z_{1R}, Z_{2R}\}$ as:

$$V_{\text{eff}}(Z_{1R}, Z_{2R}) = -\frac{1}{2}\mu_1^2 Z_{1R}^2 + \frac{g_R^4}{12\pi^2}(Z_{1R}^2)^2 - \frac{1}{2}\mu_2^2 Z_{2R}^2 + \frac{(g'_R)^4}{12\pi^2}\left(Z_{2R}^2 + \frac{2}{g'_R}Z_{2R}\cdot b\right)^2, \quad (60)$$

where we have fixed the condition $a^\mu = 0$, with the shift $B^\mu \to \frac{b^\mu}{g'_R} + Y^\mu$, and the rotation to the physical eigenstates from (50a) and (50b).

## V. NEUTRINO OSCILLATIONS IN THE DLSB SCENARIO

Since the discovery of the oscillation phenomena associated with the non-null neutrino's masses in a basis which does not match with the flavor basis of the SM, several models beyond the SM were proposed in order to explain this phenomena in the literature [32–34]. We start the description of the oscillation phenomena considering the three flavor neutrinos eigenstates $|\nu_\alpha\rangle = \{|\nu_e\rangle, |\nu_\mu\rangle, |\mu_\tau\rangle\}$. After the seesaw mechanism takes place, we define the physical eigenstates $|\nu_i\rangle$, with $i = \{1, 2, 3\}$, that represent the LHNs with light masses. These physical eigenstates are related with the previous flavor neutrinos eigenstates by the transformation

$$|\nu_i\rangle = \sum_\alpha U_{i\alpha}|\nu_\alpha\rangle, \qquad |\nu_\alpha\rangle = \sum_i U^*_{\alpha i}|\nu_i\rangle, \quad (61)$$

in which $U_{i\alpha}$ is the so-called Pontecorvo–Maki–Nakagawa–Sakata (PMNS) unitary and complex matrix. The dynamic of the physical eigenstates is ruled by the spatial-time evolution:

$$|\nu_i(\mathbf{x}, t)\rangle = e^{i(E_i t + \mathbf{p}_i\cdot\mathbf{x})}|\nu_i(0, 0)\rangle. \quad (62)$$

Therefore, the transition probability of oscillation between flavors states $|\nu_\alpha\rangle \to |\nu_\beta\rangle$ is defined by

$$P_{\alpha\to\beta}(\mathbf{x}, t) = |\langle\nu_\alpha(\mathbf{x}, t)|\nu_\beta(\mathbf{x}, t)\rangle|^2 = \left|\sum_i U^*_{i\alpha}U_{i\beta}e^{iE_i t}e^{i\mathbf{p}_i\cdot\mathbf{x}}\right|^2. \quad (63)$$

The energy of a $i$-neutrino in the physical eigenstate basis is

$$E_i = \sqrt{\mathbf{p}_i^2 + m_i^2} \simeq |\mathbf{p}_i| + \frac{m_i^2}{2|\mathbf{p}_i|} = E + \frac{m_i^2}{2E}, \quad (64)$$

where we have considered the approximation $|\mathbf{p}_i| \gg m_i$, and assuming that $t \approx x$ and $\mathbf{p}_i - \mathbf{p}_j \approx 0$, the transition probability is

$$P_{\alpha\to\beta}(x) = \delta_{\alpha\beta} - 4\sum_{\substack{i,j=1,\\ i>j}}^{3}\Re[U^*_{i\alpha}U_{i\beta}U_{\alpha j}U^*_{\beta j}]\sin^2\left[\left(\frac{\Delta m_{ij}^2}{4E}\right)x\right] + 2\sum_{\substack{i,j=1,\\ i>j}}^{3}\Im[U^*_{i\alpha}U_{i\beta}U_{\alpha j}U^*_{\beta j}]\sin\left[\left(\frac{\Delta m_{ij}^2}{2E}\right)x\right], \quad (65)$$

in which $\Re$ and $\Im$ are the real and imaginary parts of the PMNS matrix elements. The previous result (65) is associated with the usual dispersion relation for the light $i$-neutrino. Notice also that this result depends on the PMNS matrix elements, and depends on the squared difference of the mass between a $i$-physical eigenstate and a $j$-physical eigenstate, $\Delta m_{ij}^2 \coloneqq m_i^2 - m_j^2$, and the known oscillation length is $\ell_{ij} = 4\pi E/|m_i^2 - m_j^2|$.

In the case of the model with DLSB, we consider the transition probability for the neutrino dispersion relation from the phase I in (31), in which the VEV parameter is timelike, i.e., $a^\mu = (a^0, \mathbf{0})$. In this particular case, the light $i$-neutrino dispersion relation is:

$$E_i^{(\pm)} = \sqrt{||\mathbf{p}_i| \pm \mu_i|^2 + m_i^2} \simeq ||\mathbf{p}_i| \pm \mu_i| + \frac{m_i^2}{2||\mathbf{p}_i| + \mu_i|} \simeq |E \pm \mu_i| + \frac{m_i^2}{2|E \pm \mu_i|}, \quad (66)$$

where $\mu_i \coloneqq (a^0)_i = \pi\sqrt{3}(g_{1R})_i/g$ $(i = 1, 2, 3)$ means the timelike parameter for each $i$-neutrino (or $i$-antineutrino), $E_i^{(+)}$ is the energy of the light $i$-neutrino, and $E_i^{(-)}$ is the correspondent for the $i$-antineutrino. To obtain the difference of energy of a $i$-neutrino with a $j$-neutrino in this scenario, we assume $(\mu_i, \mu_j) > 0$, and with a flavor dependent on the coupling constant $(g_{1R})_i$ $(i = 1, 2, 3)$. Under these conditions, the difference of energy is

$$E_i^{(\pm)} - E_j^{(\pm)} \simeq |E \pm \mu_i| - |E \pm \mu_j| + \frac{m_i^2}{2|E \pm \mu_i|} - \frac{m_j^2}{2|E \pm \mu_j|}$$
$$\approx \pm(\mu_i - \mu_j) + \frac{\Delta m_{ij}^2}{2E}, \tag{67}$$

where we have used $E \gg (\mu_i, \mu_j)$ in the last line. Notice that this result yields different oscillation lengths for the neutrino and antineutrino induced by the DLSB violation.

To simplify our future estimate, we reduce our problem for the case of the transition probability of muon and electron neutrinos. Thereby, the PMNS matrix is reduced in terms of the electron-muon mixing angle $\theta_{12}$:

$$\begin{pmatrix} \nu_1 \\ \nu_2 \end{pmatrix} = \begin{bmatrix} \cos\theta_{12} & \sin\theta_{12} \\ -\sin\theta_{12} & \cos\theta_{12} \end{bmatrix} \begin{pmatrix} \nu_e \\ \nu_\mu \end{pmatrix}, \tag{68}$$

where $\sin^2\theta_{12} = 0.307 \pm 0.013$ [35]. The probability of the $\nu_e$-neutrino changes its flavor to $\nu_\mu$ is read below:

$$P_{\nu_e \to \nu_\mu}(x) = \sin^2(2\theta_{12})\sin^2\left[(E_1^{(+)} - E_2^{(+)})\frac{x}{2}\right]$$
$$= \sin^2(2\theta_{12})\sin^2\left(\frac{\pi x}{\ell}\right), \tag{69}$$

in which the correspondent oscillation length $\ell$ is

$$\ell^{-1} = \left|\frac{\pi\sqrt{3}}{2g}(\Delta g_{1R})_{12} + \frac{\Delta m_{12}^2}{4\pi E}\right|, \tag{70}$$

where $(\Delta g_{1R})_{12} \coloneqq (g_{1R})_1 - (g_{1R})_2$, and the difference of squared masses is in the range $\Delta m_{12}^2 = 10^{-2}$–$10^{-3}$ eV$^2$ for experiments in accelerators [35]. The usual oscillation length in the literature is recovered when $(g_1)_i \to 0$. For a strong coupling regime (SCR) $(\Delta g_{1R})_{12} \gg \Delta m_{12}^2/E$, we obtain

$$\ell^{-1} \simeq \pi\frac{\sqrt{3}}{2}\left|\frac{(\Delta g_{1R})_{12}}{g}\right|. \tag{71}$$

The transition probability $P_{\nu_e \to \nu_\mu}$ is illustrated as a function of $x$ in Fig. 2, and posteriorly, it is also illustrated as function of energy ($E$) in Fig. 3, respectively. In both plots, we have used the $\Delta m_{12}^2 = 0.041$ eV$^2$ and $\sin^2(2\theta_{12}) = 0.96$ [36]. In the Fig. 2, we have chosen the values $(\Delta g_{1R})_{12}/g = 0$ (black line), $(\Delta g_{1R})_{12}/g = +0.1$ meV (red line) and $\Delta G = -0.1$ meV (blue line), in energy ($E$) units. In fig. (3), we have chosen $(\Delta g_{1R})_{12}/g = 0$ (black line), $(\Delta g_{1R})_{12}/g = 0.2$ eV (red line), and $(\Delta g_{1R})_{12}/g = -0.2$ eV (blue line). The graphics show that the effect of the DLSB in the neutrino oscillation is greater for large energy values.

As can be seen in Fig. 2, the DLSB effect is to shift the transition probability in the $x$-axis. Notice that, in Fig. 3, the

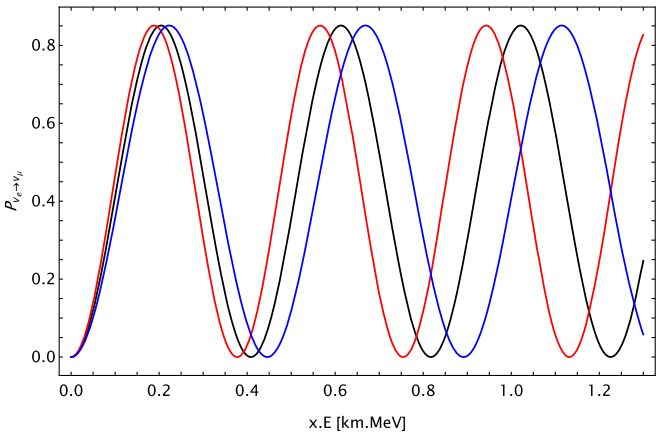


FIG. 2. The transition probability $P_{\nu_e \to \nu_\mu}$ as function of the distance $x$ in energy ($E$) units. We use $\Delta m_{12}^2 = 0.041$ eV$^2$ and $\sin^2(2\theta_{12}) = 0.96$, for the values $(\Delta g_{1R})_{12}/g = 0$ (black line), $(\Delta g_{1R})_{12}/g = 0.1$ meV (red line), and $(\Delta g_{1R})_{12}/g = -0.1$ meV (blue line).

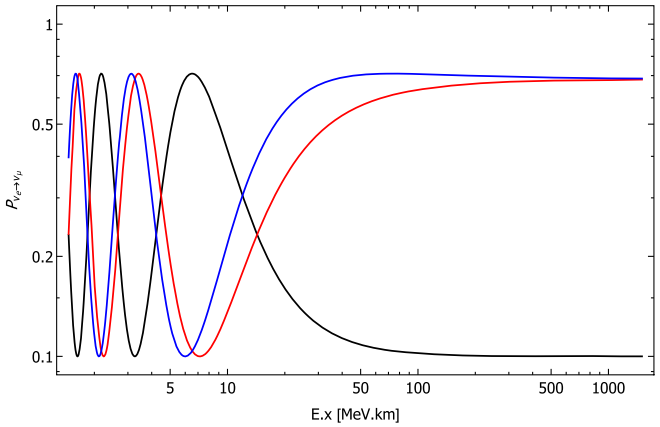


FIG. 3. The transition probability $P_{\nu_e \to \nu_\mu}$ as function of the energy ($E$). We also choose $\Delta m_{12}^2 = 0.041$ eV$^2$ and $\sin^2(2\theta_{12}) = 0.96$, for the values $(\Delta g_{1R})_{12}/g = 0$ (black line), $(\Delta g_{1R})_{12}/g = 0.2$ eV (red line), and $(\Delta g_{1R})_{12}/g = -0.2$ eV (blue line).

effect of the DLSB in the neutrino oscillation is to generate oscillation even for high energies, in opposition to the usual result (black line). The red (neutrinos) and blue (antineutrinos) lines also show oscillation, but the curves go to a finite value of probability that is contributed by the DLSB parameter. For large energy, the oscillation length is given by (71). If we consider $(\Delta g_{1R})_{12}/g = \pm 0.2$ eV, the transition probability limit $(E \cdot x \gg 1)$ in the red and blue curves from Fig. 3 is

$$P_{\nu_e \to \nu_\mu}(E \cdot x \gg 1) \approx 0.65. \tag{72}$$

Going further, in Fig. 4, we show the allowed region in the parameter space of $\sin^2(2\theta_{12})$ versus $\Delta m_{12}^2$. Based on an oscillation probability of $P_{\nu_e \to \nu_\mu} = (2.6 \pm 1.5) \times 10^{-3}$

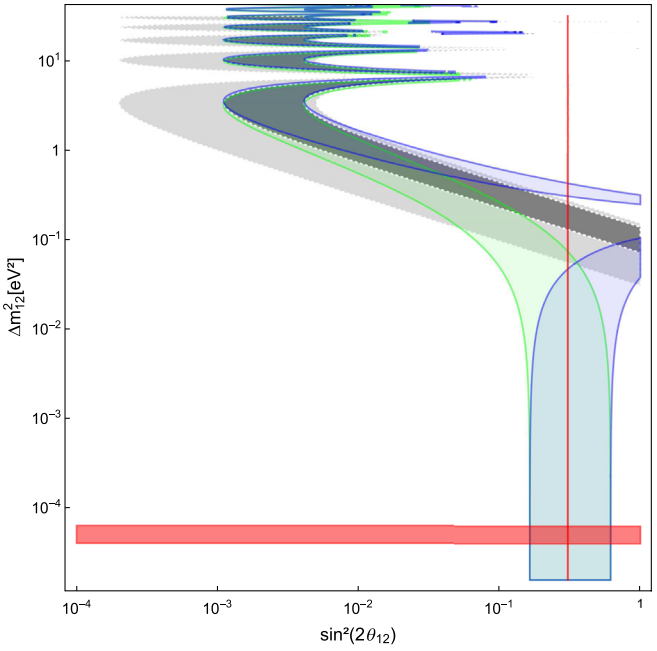


FIG. 4. The parameter space of $\sin^2(2\theta_{12})$ versus $\Delta m^2_{12}$ for the electron-neutrino oscillation. The gray region shows the region with 68% confidence level and the light gray shows the region for the 95% confidence level, according to the LSND experiment. The green and blue regions shows the allowed region for $(\Delta g_{1R})_{12}/g = 10^{-9}$ eV and $(\Delta g_{1R})_{12}/g = -10^{-9}$ eV based on the LSND result (68% C.L.). The red region indicates the region with 68% confidence level from the Super-Kamiokande experiment [35].

from the LSND experiment [2], and using $E =$ 60–200 MeV and $x = L \approx 30$ m $= 2.4 \times 10^7$ eV$^{-1}$, we plot the range of $\sin^2(2\theta_{12})$ and $\Delta m^2_{12}$ values compatible with this result (gray and light gray regions in Fig. 4, for 68% C.L. and 95% C.L., respectively). Based on the phenomenological bounds from [16], we consider $(\Delta g_{1R})_{12}/g \approx \pm 10^{-10}$ eV, and plotting their contribution in the probability one can see in the Fig. 4 where the green and blue regions are in contact with long base line (LBL) accelerators results (interception of the red regions), in contrast to the symmetric case (gray regions). It happens due to the smallness of the argument $\frac{\Delta m^2_{12}}{4\pi E}$, since that $\frac{\Delta m^2_{12}}{4\pi E} \approx 10^{-12}$ eV. Thereby, the contribution of the mass splitting and DLSB parameter is small and obeys the hierarchy condition $\frac{\pi\sqrt{3}}{2g}(\Delta g_{1R})_{12} > \frac{\Delta m^2_{12}}{4\pi E}$, such way the oscillation length in the Eq. (71) can be rewritten as $\frac{1}{\ell} \approx \frac{\sqrt{3}\pi}{2g}(\Delta g_{1R})_{12}$. Finally, one can note that $L/\ell < 1$, and due to this property, one can approximate the oscillation probability as:

$$P^{\mathrm{SCR}}_{\nu_e \to \nu_\mu} \approx \frac{3\pi^4}{8}\sin^2(2\theta_{12})\left[L\frac{(\Delta g_{1R})_{12}}{g}\right]^2, \qquad (73)$$

and using the PDG best fit for $\sin^2(2\theta_{12}) \approx 0.31$ and $L \approx 30$ m, one finds:

$$P^{\mathrm{SCR}}_{\nu_e \to \nu_\mu} \approx 6.5 \times 10^{15}\left[\frac{(\Delta g_{1R})_{12}}{g}\right]^2 = (2.6 \pm 1.5) \times 10^{-3}. \qquad (74)$$

Therefore, one can infer that $|\frac{(\Delta g_{1R})_{12}}{g}| = 8 \times 10^{-19}$ GeV with 68% C.L., the same order of magnitude of the bounds from the tandem model [17], and consistent with our initial assumptions.

## VI. CONCLUSIONS

A model with two massive Majorana fermions coupled through self-quartic interactions themselves was proposed in this paper. After a type-II seesaw mechanism, one of the Majorana fermions acquires a light mass ($m_1$), the other one gains a heavy mass ($m_2$), and we obtain an effective model with quartic self-interaction fermion theory of axial currents in the physical basis. The model allows the introduction of two auxiliary gauge fields in which the effective potential has a minimum at two vacuum expected values (VEVs) that are constant 4-vectors. These VEVs scales break dynamically the Lorentz symmetry of the model, and as consequence, the dispersion relations of the Majorana fermions are modified.

We calculate the correspondent frequencies solutions for the light and heavy Majorana fermions in the scenarios of timelike and spacelike 4-vectors. Posteriorly, we analyze the fluctuations of the auxiliary gauge fields around the VEV scales to calculate the effective action expanded up to second order. Therefore, the radiative corrections yield kinetic terms and mixed mass terms for the gauge fields. The mass matrix is so diagonalized, where the physical eigenstates have one mass of $M_{Z_{1R}} \approx \sqrt{6}m_1$ for the light gauge field ($Z_{1R}$), and a mass of $M_{Z_{2R}} \approx \sqrt{6}m_2$ for the heavy gauge field ($Z_{2R}$). Since we just consider one DLSB parameter, the radiative corrections also generate the Chern-Symons term associated with the heavy gauge field. Using the field equations, we obtain the dispersion relations and the frequency solutions for the gauge fields on a diagonal basis.

To end, we investigate the DLSB in the neutrino's oscillation. The dispersion relation obtained previously for the light Majorana fermions is used to calculate the transition probability $\nu_e \to \nu_\mu$ and the length oscillation. It is well known that the neutrino oscillation in the electron-muon sector measured by Super-Kamiokande experiment [37] differs from the LSND [2,3] and the MiniBooNe experiments 36]], as can be seen in Fig. 1, where one plots the parameter space of $\sin^2(2\theta_{12})$ versus $\Delta m^2_{12}$. The allowed region for the LSND and the Super-Kamiokande experiments can be seen as the red and gray regions of Fig. 1, respectively. The blue and green regions represents the allowed phase space with

the contribution of the DLSB parameter with approximate value of $\frac{(\Delta g_{1R})_{12}}{g} \approx \pm 6 \times 10^{-19}$ GeV on the DLSB parameter.

As can be seen in Fig. 1, if we admit the light and heavy sector interacts through the axial channel ($G_3 \neq 0$) only one of the sectors violates dynamically the Lorentz symmetry, and the VEVs scales are given by

$$a^2 = \frac{3\pi^2 G_2}{G_1 G_2 - G_3^2} \quad \text{and} \quad b^2 = 0, \tag{75}$$

or

$$a^2 = 0 \quad \text{and} \quad b^2 = \frac{3\pi^2 G_1}{G_1 G_2 - G_3^2}, \tag{76}$$

where $a^\mu$ and $b^\mu$ couple with the light and heavy sectors, respectively. Thereby, there is a possibility in the phase diagram for the DSLB occurs in the heavy sector maintaining the standard model of the symmetric sector under Lorentz symmetry. One also has that for $G_3 = 0$, i.e., in the decoupled scenario, both the VEVs scales can be non-null simultaneously.

If one assumes $G_3 = 0$, i.e., the light neutrino sector decouples from the heavy sector, one can estimate the Lorentz violation parameter in the axial neutrino self-interaction. The authors choose this framework since the heavy sector up to date was not detected, which indicates that, if it exists, the heavy sector interacts weakly with the SM particles, particularly with neutrinos. Using the SME limits from $a_e^0 = |(a_L)^T_{ee}| < 2 \times 10^{-27}$ GeV (from Table D29 of Ref. [38]), we obtain the upper bound:

$$|(a_L)^T_{\mu\mu}| \lesssim 3 \times 10^{-18} \text{ GeV}, \tag{77}$$

which means the muonic neutrino sector would be the relevant sector in the axial quartic interactions. Based on the experimental results from oscillations of muonic neutrinos [39,40], which reveals no discrepancies with the standard neutrino oscillation models, one can roughly assume the following hierarchy:

$$|(a_L)^T_{ee}| \ll |(a_L)^T_{\mu\mu}| \approx |(a_L)^T_{\tau\tau}|. \tag{78}$$

Is important to comment on the case $G_3 \neq 0$: If one assumes a more general statement that the light and heavy sectors interact through $G_3$, the analysis become much more complex. In fact, any attempt to find any bound assuming $G_3 \neq 0$ becomes unfeasible with the actual experimental data. In addition to the fact that $G_2$ and $G_3$ are constants related to the heavy sector (which one has no information about) more general assumptions should be made, i.e., the full flavor structure of the quartic interactions. These features will be studied in other opportunities.

From the phenomenological point of view, in the high energy limit, the quantity $\Delta m^2/E$ vanishes and implies that neutrinos at high energy do not oscillate. In the case of DLSB, the oscillation remains even in the high energy limit and can be a motivation to search for oscillation patterns in events from natural astrophysical phenomena which produce particles with energy beyond the PeV scale [41,42].

Going further, since $|a^0| \propto G_1^{-1/2}$, one can roughly estimate the coupling constant for the muon and tau neutrinos: $G_1^{(\mu)} \approx G_1^{(\tau)} \approx 10^{34}$ GeV$^{-2}$. In such a strong coupling environment nonperturbative phenomena may take place and nonlinear aspects could drive the system [30]. The effects of this kind of interaction also could be tested in the context of supernova processes and could also generate cosmological implications. These new features will be research subjects in forthcoming papers.

## ACKNOWLEDGMENTS

Y. M. P. G. is supported by a postdoctoral grant from Fundação Carlos Chagas Filho de Amparo à Pesquisa do Estado do Rio de Janeiro (FAPERJ). M. J. Neves thanks CNPq (Conselho Nacional de Desenvolvimento Científico e Tecnológico), Brazilian scientific support federal agency, for partial financial support, Grant No. 313467/2018-8.

[1] T. Araki *et al.* (KamLAND Collaboration), Measurement of Neutrino Oscillation with KamLAND: Evidence of Spectral Distortion, Phys. Rev. Lett. **94**, 081801 (2005).

[2] C. Athanassopoulos *et al.* (LSND Collaboration), Evidence for $\bar{\nu}_\mu \to \bar{\nu}_e$ Oscillations from the LSND Experiment at the Los Alamos Meson Physics Facility, Phys. Rev. Lett. **77**, 3082 (1996).

[3] C. Athanassopoulos *et al.* (LSND Collaboration), Results on $\nu_\mu \to \nu_e$ Neutrino Oscillations from the LSND Experiment, Phys. Rev. Lett. **81**, 1774 (1998).

[4] G. Mention, M. Fechner, Th. Lasserre, Th. A. Mueller, D. Lhuillier, M. Cribier, and A. Letourneau, The reactor antineutrino anomaly, Phys. Rev. D **83**, 073006 (2011).

[5] A. Aguilar *et al.*, Evidence for neutrino oscillations from the observation of electron anti-neutrinos in a muon anti-neutrino beam, Phys. Rev. D **64**, 112007 (2001).

[6] M. V. Smirnov, Zh. J. Hu, J. J. Ling, Yu. N. Novikov, Z. Wang, and G. Yang, Sterile neutrino oscillometry with Jinping, Eur. Phys. J. C **80**, 609 (2020).

[7] A. A. Aguilar-Arevalo *et al.* (MiniBooNE Collaboration), A combined $\nu_\mu \to \nu_e$ & $\bar{\nu}_\mu \to \bar{\nu}_e$ oscillation analysis of the MiniBooNE excesses, arXiv:hep-exp/1207.4809.

[8] Geoffrey B. Mills (LSND Collaboration), Neutrino oscillation results from LSND, Nucl. Phys. B, Proc. Suppl. **91**, 198 (2001).

[9] K. Abe *et al.*, Solar neutrino measurements in Super-Kamiokande-IV, Phys. Rev. D **94**, 052010 (2016).

[10] P. Minkowski, $\mu \to e\gamma$ at a rate of one out of $10^9$ muon decays?, Phys. Lett. **67B**, 421 (1977).

[11] R. N. Mohapatra and G. Senjanović, Neutrino Mass and Spontaneous Parity Nonconservation, Phys. Rev. Lett. **44**, 912 (1980).

[12] R. N. Mohapatra and G. Senjanovic, Neutrino Masses and Mixings in Gauge Models with Spontaneous Parity Violation, Phys. Rev. D **23**, 165 (1981).

[13] T. Yanagida, Horizontal gauge symmetry and masses of neutrinos, Conf. Proc. C **7902131**, 95 (1979).

[14] M. Gell-Mann, P. Ramond, and R. Slansky, Complex spinors and unified theories, Conf. Proc. C **790927**, 315 (1979).

[15] S. L. Glashow, The future of elementary particle physics, in *Quarks and Leptons*, edited by M. Lévy, J. L. Basdevant, D. Speiser, J. Weyers, R. Gastmans, and M. Jacob, NATO Advanced Study Institutes Series Vol. 61 (Springer, Boston, MA, 1980), 10.1007/978-1-4684-7197-7_15.

[16] Kostelecký, V. Alan, and Matthew Mewes, Lorentz and *CPT* violation in neutrinos, Phys. Rev. D **69**, 016005 (2004).

[17] Teppei Katori, Alan Kostelecky, and Rex Tayloe, Global three-parameter model for neutrino oscillations using Lorentz violation, Phys. Rev. D **74**, 105009 (2006).

[18] J. S. Diaz and V. Alan Kostelecký, Lorentz-and *CPT*-violating models for neutrino oscillations, Phys. Rev. D **85**, 016013 (2012).

[19] T. P. Cheng and L. F. Li, *Gauge Theory of Elementary Particle Physics* (Oxford University Press, New York, 1994).

[20] Baruch Rosenstein, Brian J. Warr, and Seon H. Park, Dynamical symmetry breaking in four-fermion interaction models, Phys. Rep. **205**, 59 (1991).

[21] Kiyoshi Higashijima, Theory of dynamical symmetry breaking, Prog. Theor. Phys. Suppl. **104**, 1 (1991).

[22] M. Pérez-Victoria, Exact Calculation of the Radiatively Induced Lorentz and *CPT* Violation in QED, Phys. Rev. Lett. **83**, 2518 (1999).

[23] V. A. Miransky, *Dynamical Symmetry Breaking in Quantum Field Theories* (World Scientific, Singapore, 1994).

[24] Y. Nambu and G. Jona-Lasinio, Dynamical model of elementary particles based on an analogy with superconductivity, Phys. Rev. **122**, 345 (1961).

[25] M. Gomes, T. Mariz, J. R. Nascimento, and A. J. da Silva, Dynamical Lorentz and *CPT* symmetry breaking in a 4D four-fermion model, Phys. Rev. D **77**, 105002 (2008).

[26] J. F. Assunção, T. Mariz, J. R. Nascimento, and A. Y. Petrov, Dynamical Lorentz symmetry breaking in a 4D massless four-fermion model, Phys. Rev. D **96**, 065021 (2017).

[27] J. F. Assunção, T. Mariz, J. R. Nascimento, and A. Y. Petrov, Dynamical Lorentz symmetry breaking in a tensor bumblebee model, Phys. Rev. D **100**, 085009 (2019).

[28] J. F. Assunção, T. Mariz, J. R. Nascimento, and A. Y. Petrov, Induced Chern-Simons modified gravity at finite temperature, J. High Energy Phys. 08 (2018) 072.

[29] B. Charneski, M. Gomes, T. Mariz, J. R. Nascimento, and A. J. da Silva, Dynamical Lorentz symmetry breaking in 3D and charge fractionalization, Phys. Rev. D **79**, 065007 (2009).

[30] Y. M. P. Gomes, Dyson-Schwinger equation approach to Lorentz symmetry breaking with finite temperature and chemical potential, Phys. Rev. D **104**, 015022 (2021).

[31] Sean M. Carroll, George B. Field, and Roman Jackiw, Limits on a Lorentz- and parity-violating modification of electrodynamics, Phys. Rev. D **41**, 1231 (1990).

[32] Shinya Kanemura, Toshinori Matsui, and Hiroaki Sugiyama, Neutrino mass and dark matter from gauged $U(1)_{B-L}$ breaking, Phys. Rev. D **90**, 013001 (2014).

[33] Pilar Coloma, M. C. Gonzalez-Garciab, and Michele Maltoni, Neutrino oscillation constraints on $U(1)'$ models: From non-standard interactions to long-range forces, J. High Energy Phys. 01 (2021) 114.

[34] Cesar Bonilla, Leon M. G. de la Vega, R. Ferro-Hernandez, Newton Nath, and Eduardo Peinado, Neutrino phenomenology in a left-right $D4$ symmetric model, Phys. Rev. D **102**, 036006 (2020).

[35] P. A. Zyla *et al.* (Particle Data Group), Review of Particle Physics, Prog. Theor. Exp. Phys. **2020**, 083C01 (2020).

[36] A. A. Aguilar-Arevalo *et al.* (MiniBooNE Collaboration), Significant Excess of Electronlike Events in the MiniBooNE Short-Baseline Neutrino Experiment, Phys. Rev. Lett. **121**, 221801 (2018).

[37] Y. Fukuda *et al.* (Super-Kamiokande Collaboration), Evidence for Oscillation of Atmospheric Neutrinos, Phys. Rev. Lett. **81**, 1562 (1998).

[38] V. Kostelecký and N. Russell, Data tables for Lorentz and *CPT* violation, Rev. Mod. Phys. **83**, 11 (2011).

[39] P. Adamson *et al.* (MINOS+ Collaboration), Precision Constraints for Three-Flavor Neutrino Oscillations from the Full MINOS+ and MINOS Dataset, Phys. Rev. Lett. **125**, 131802 (2020).

[40] M. G. Aartsen *et al.* (IceCube Collaboration), Determining neutrino oscillation parameters from atmospheric muon neutrino disappearance with three years of IceCube DeepCore data, Phys. Rev. D **91**, 072004 (2015).

[41] M. G. Aartsen *et al.* (IceCube Collaboration), First Observation of PeV-Energy Neutrinos with IceCube, Phys. Rev. Lett. **111**, 021103 (2013).

[42] IceCube Collaboration, Detection of a particle shower at the Glashow resonance with IceCube, Nature (London) **591**, 220 (2021).